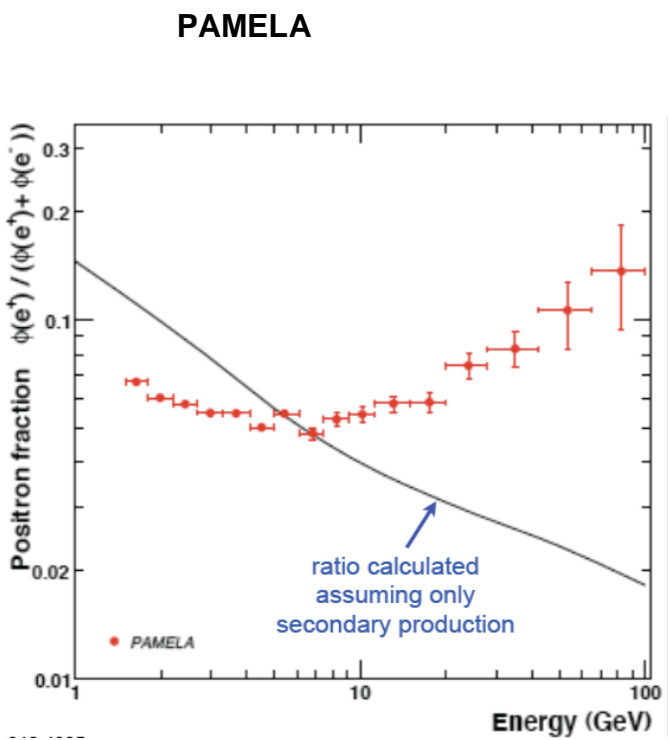
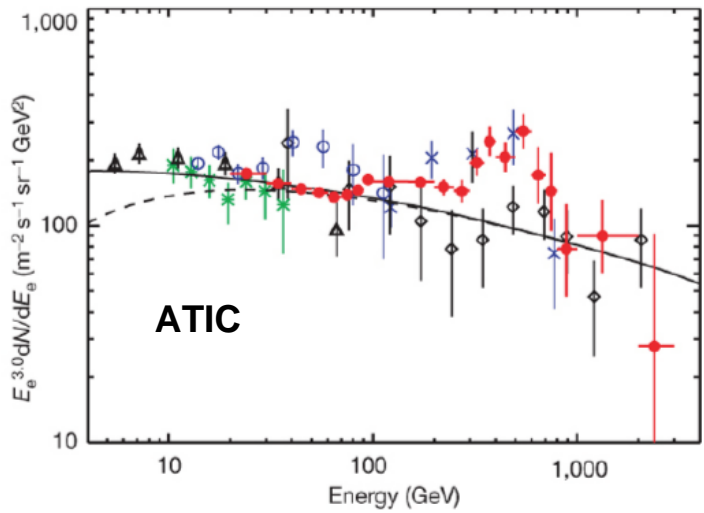
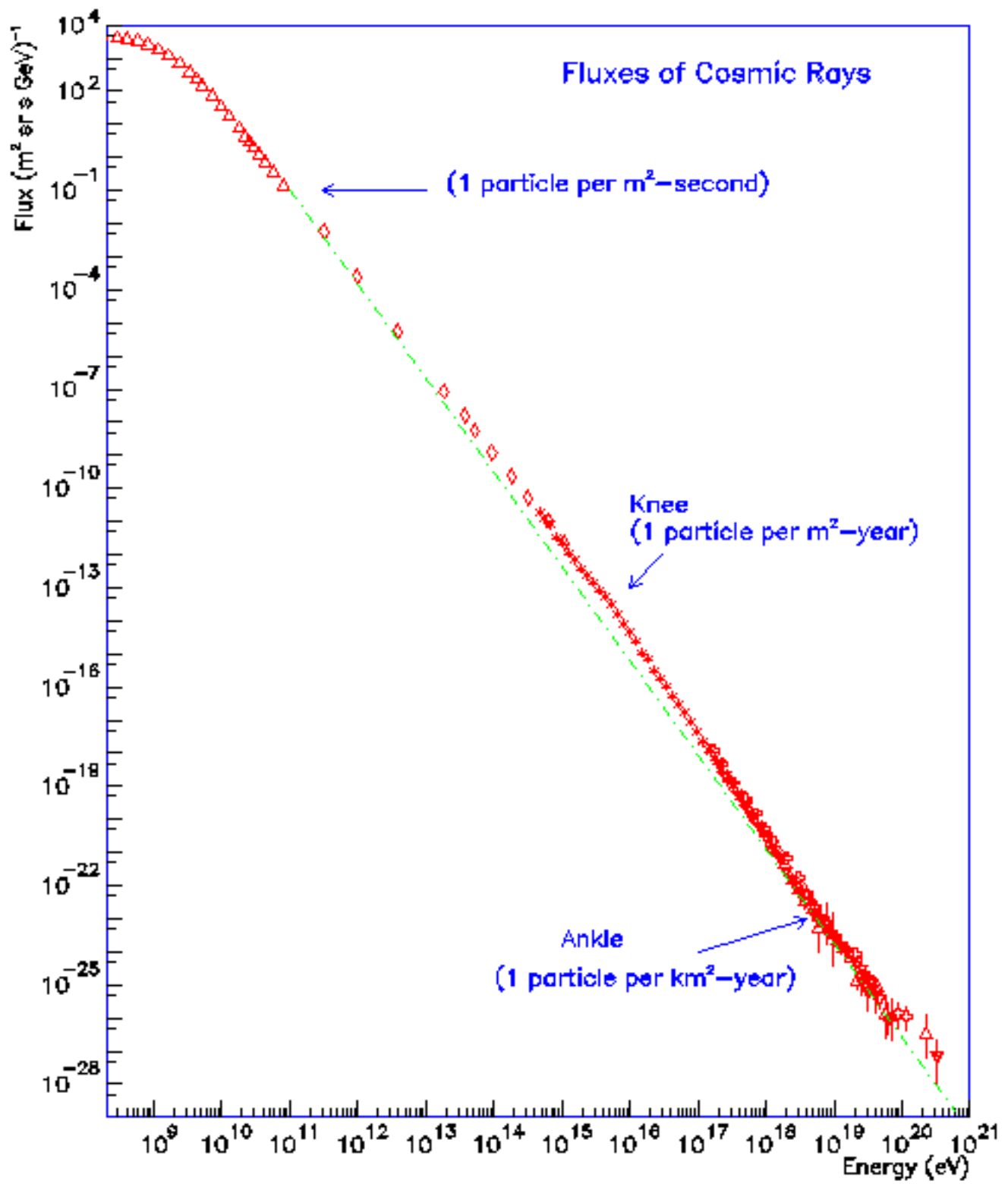


Fig. 1.1. The ionization as a function of the depth in the atmosphere. The diamonds are from the flight of Kohlhörster and the circles and asterisks are from the underwater measurements of Millikan.





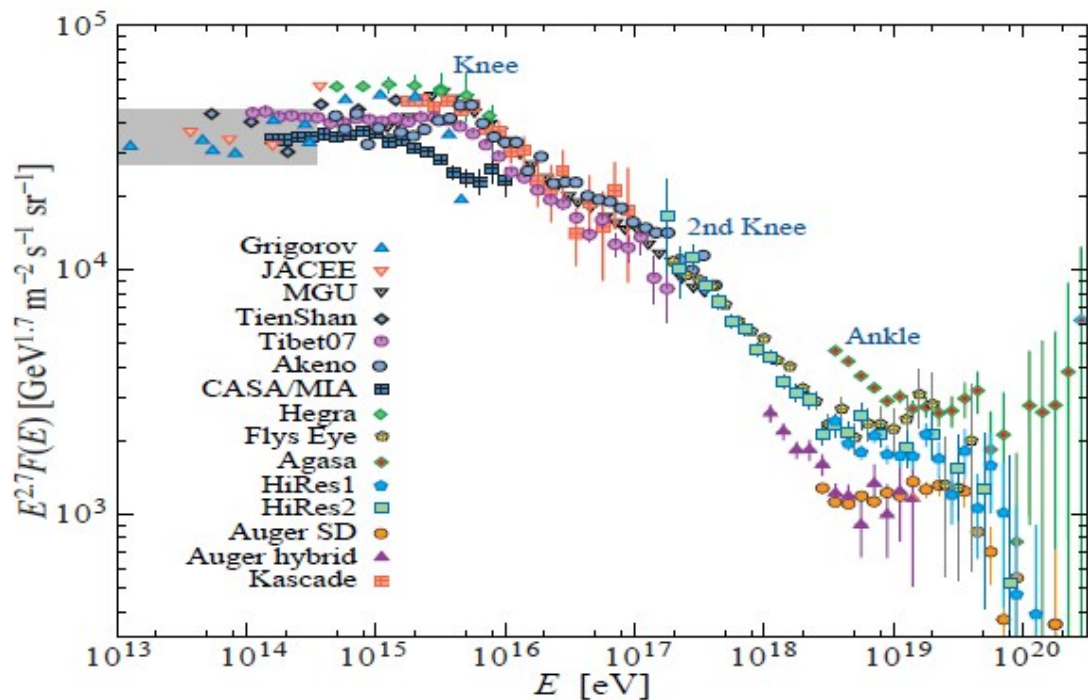
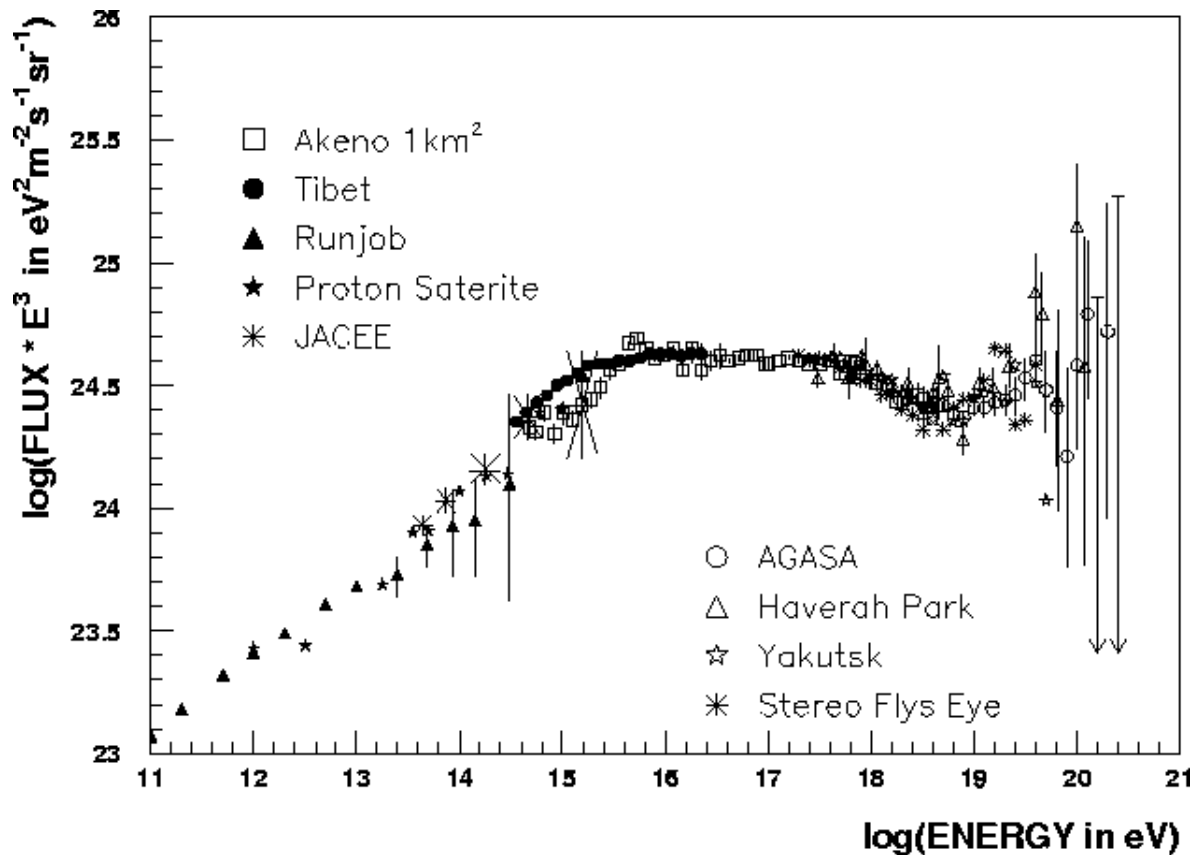
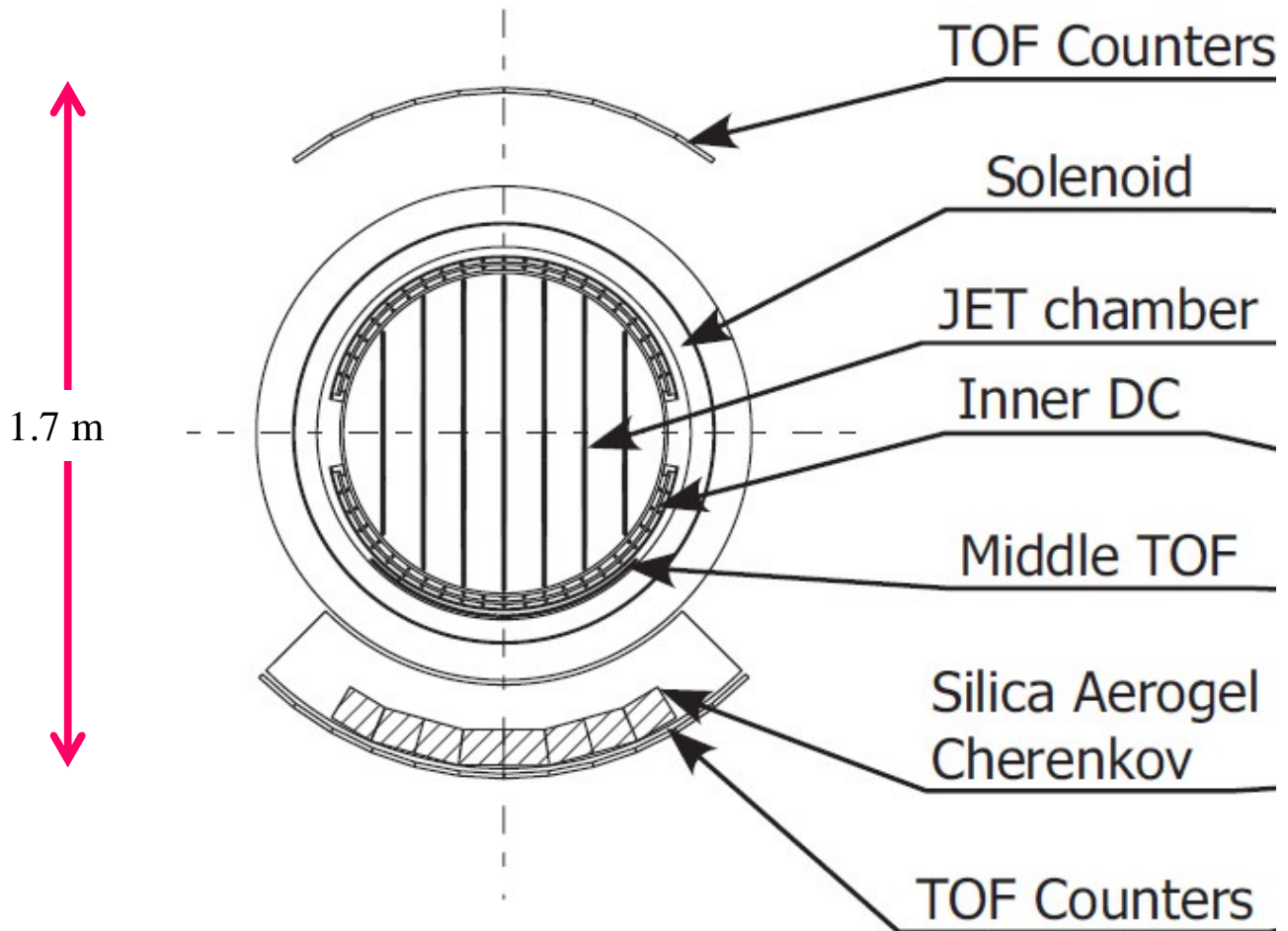


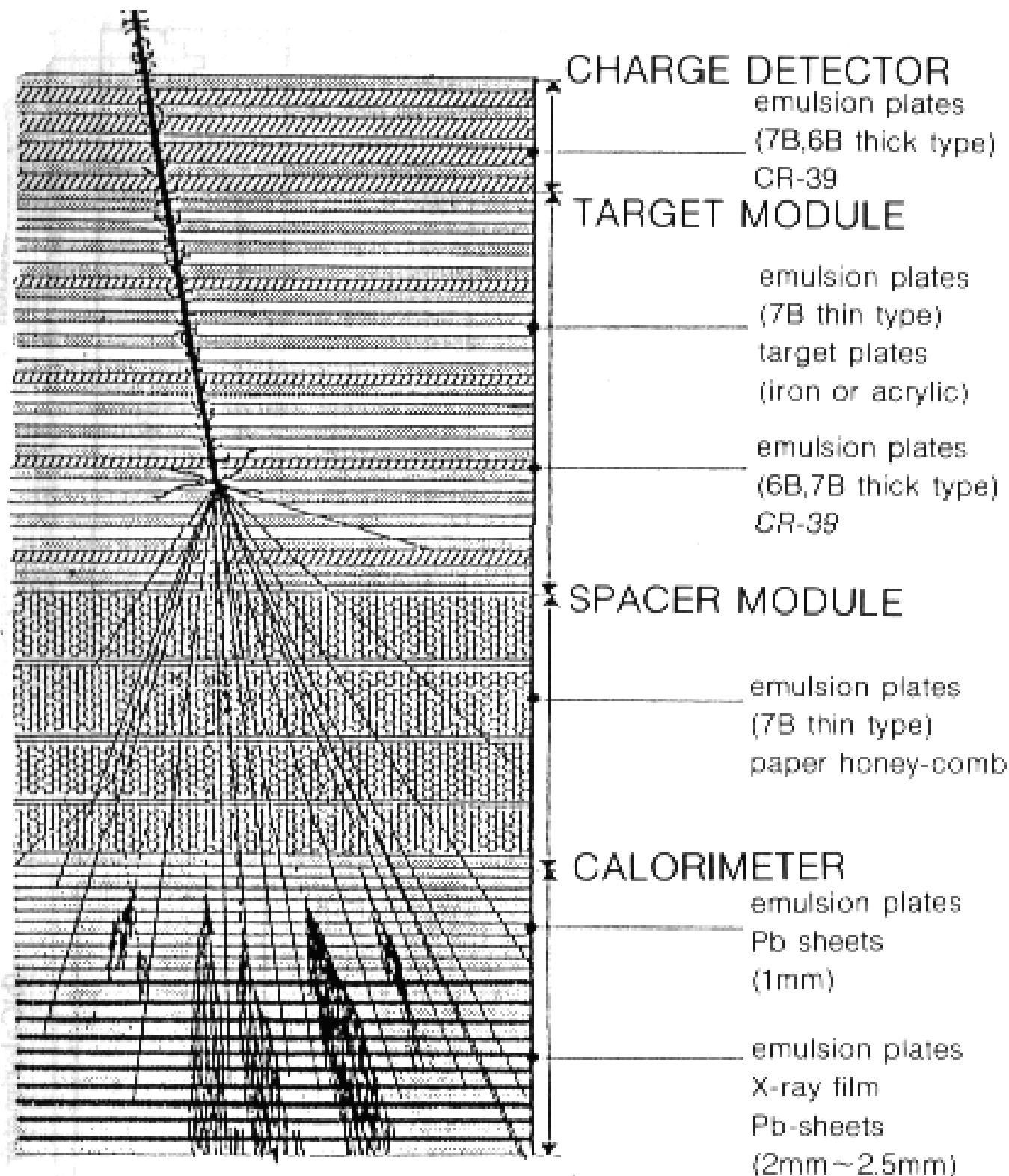
Figure 2.2: The high energy, all-particle cosmic ray spectrum multiplied by  $E^{2.7}$  for indirect experiments, demonstrating the rather substantial spread in the data. The grey band shows the reach of direct detection experiments as of 2008. [4]

## BESS – Balloon-born Experiment with Superconducting Spectrometer



- ToF Counters                      scintillatori, misurano tempi e perdita di energia
- Solenoid                            generatore del campo magnetico (1 Tesla)
- JET chamber                        tracciatore centrale con camera a drift, in campo magnetico
- Inner DC                            camere a drift interne
- Silica Aerogel Cherenkov        rivelatore Cherenkov

# JACEE



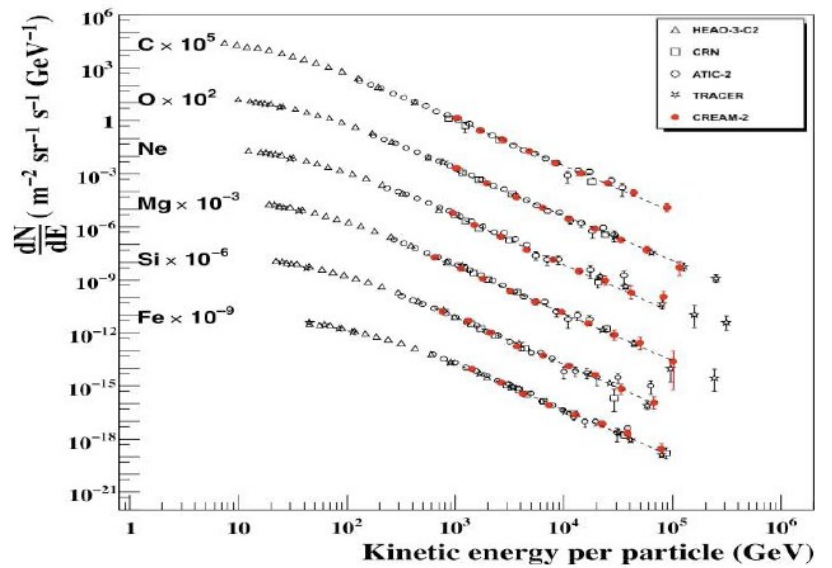
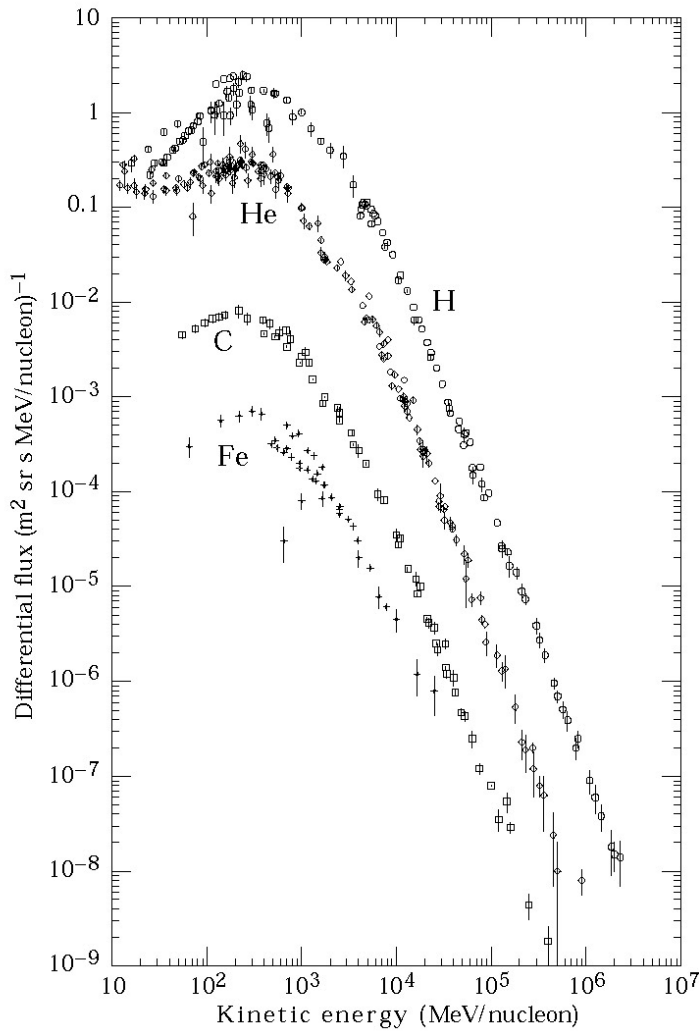


Figure 5.3: Red circles denote the spectra measured by CREAM II for the primary cosmic ray nuclei: Carbon, Oxygen, Neon, Magnesium, Silicon, and Iron. The data are consistent with both the space-based HEAO and CRN measurements and TRACER and ATIC 2, two other balloon-born instruments utilizing different detection techniques. The dashed lines represent power law fits to the CREAM data.

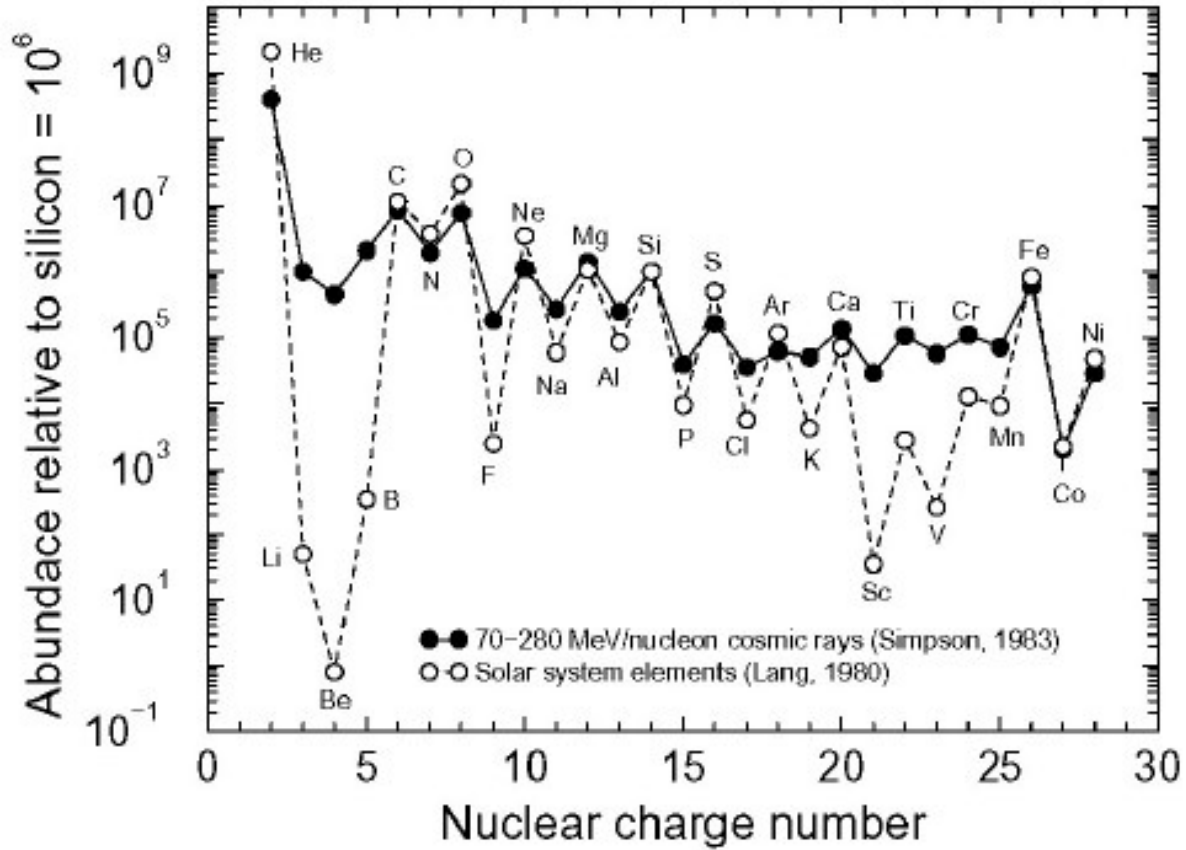


Fig. 2.— The relative elemental abundances of 70-280 MeV/nucleon cosmic rays (closed circles, taken from Tab. 2 by Simpson, 1983) compared to the solar system abundances (open circles, taken from Tab. 38 by Lang, 1980) normalized to Si =  $10^6$ .

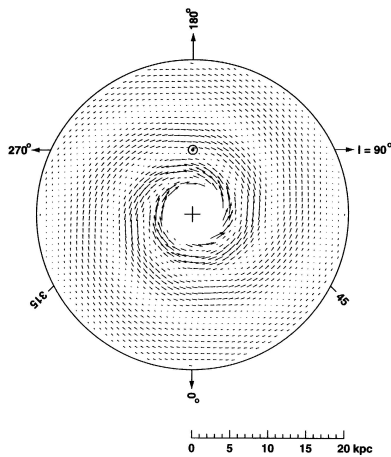
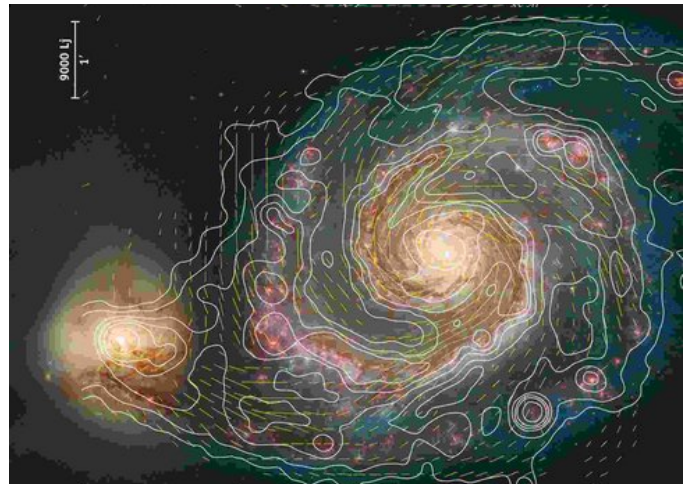
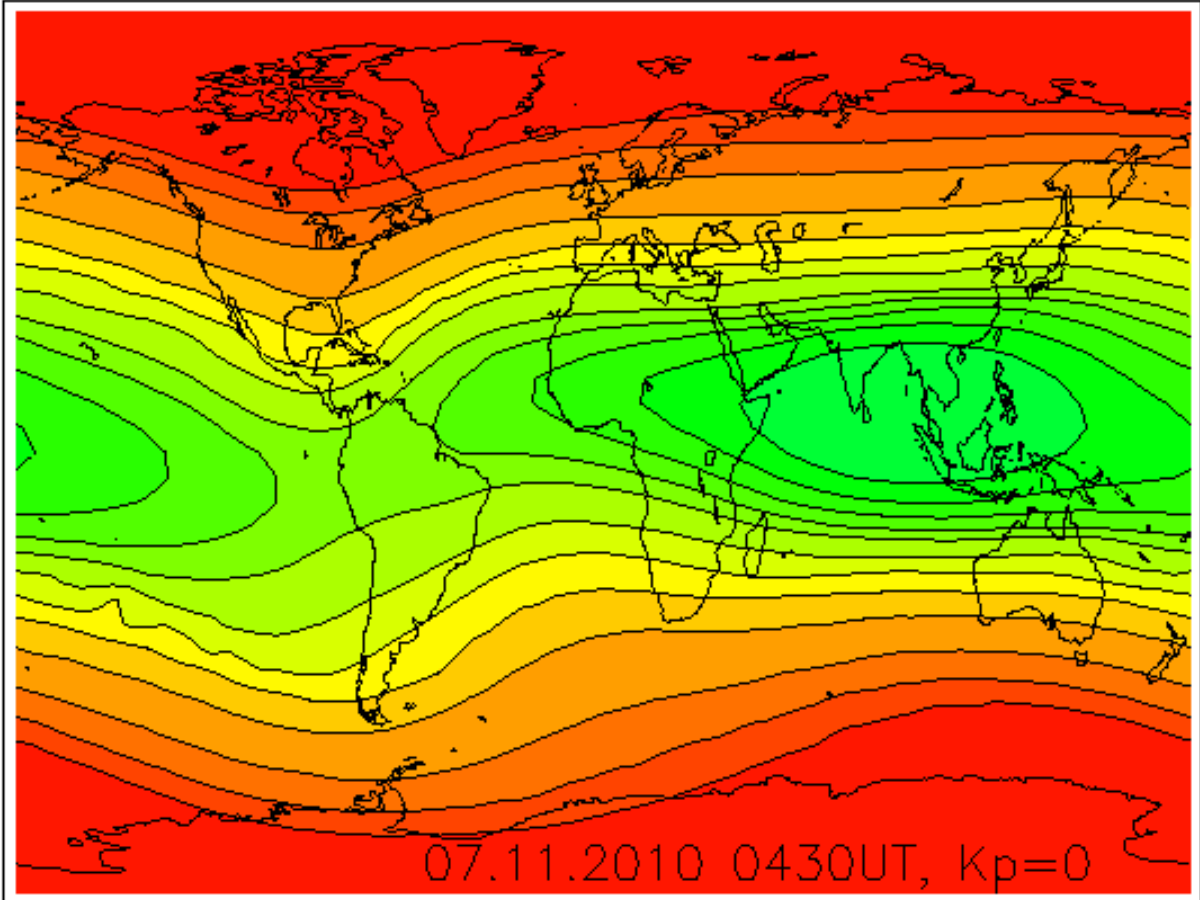


Fig. 4.4. Magnetic field strength (length of arrows) and direction in the galactic plane for the BSS model [76]. The field reversals can be best seen close to the galactic center where the field values are higher. The field is not plotted within 4 kpc of the galactic center because of the very high uncertainty in this region. The positions of the galactic center and the solar system are indicated.



Campo magnetico di una galassia simile alla via Lattea



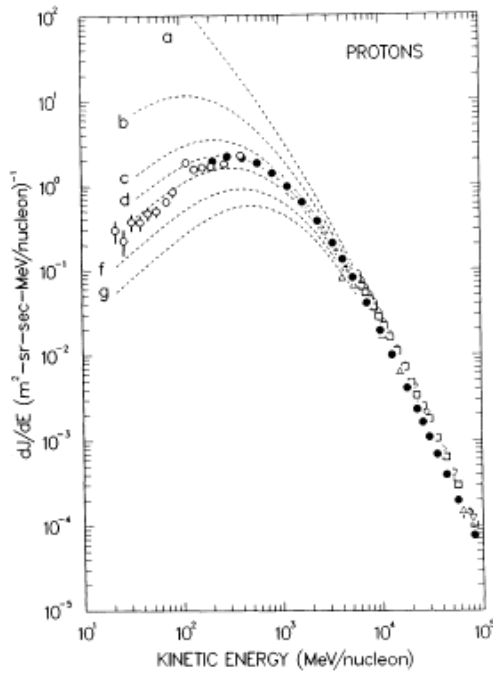


FIG. 9a

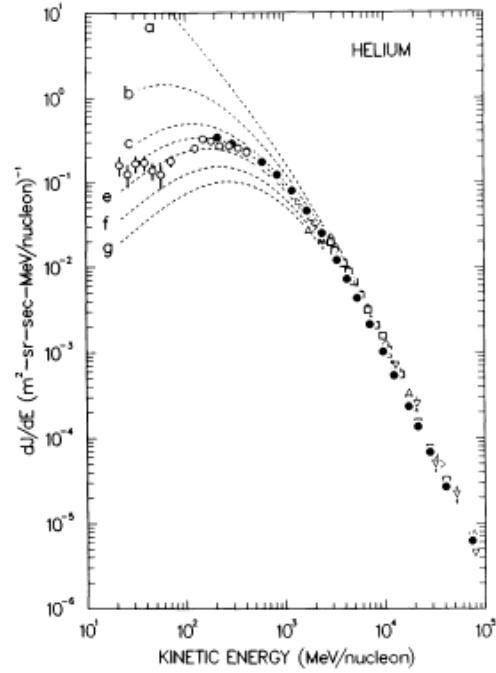
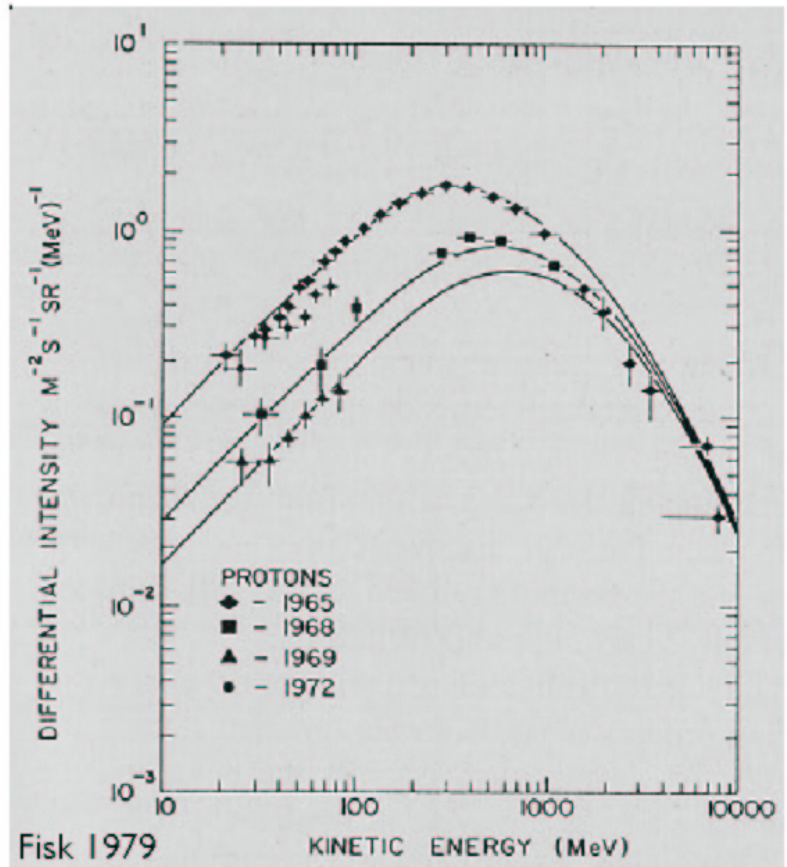
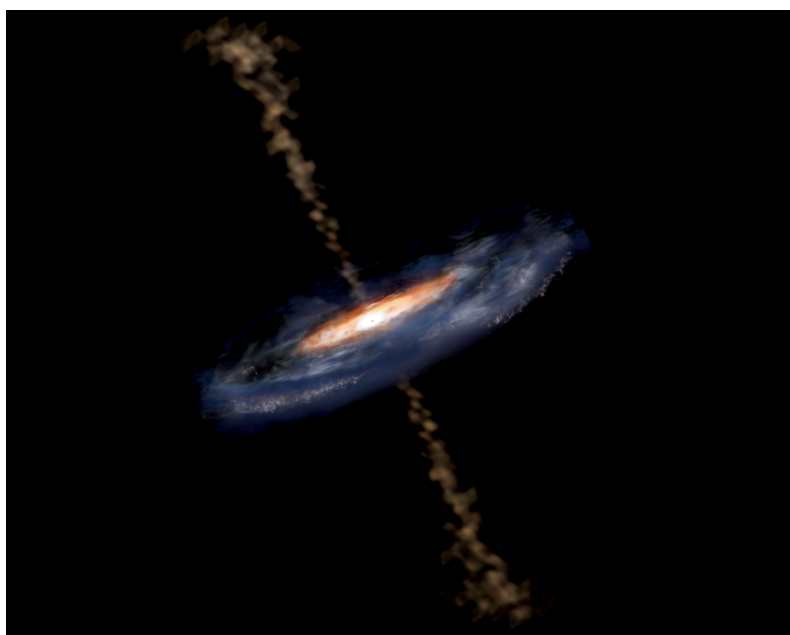
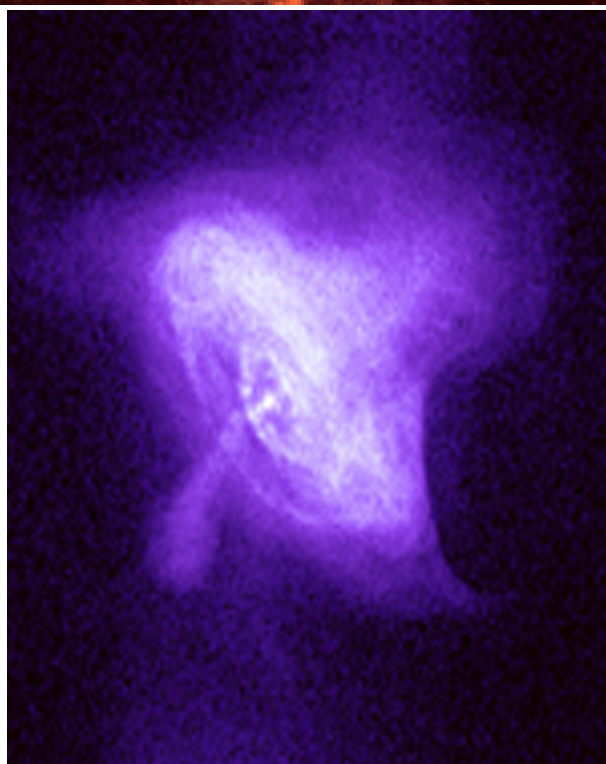
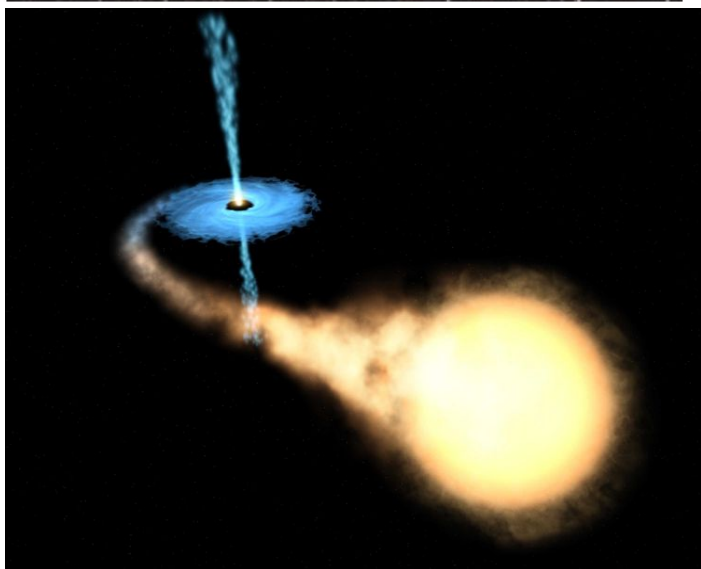
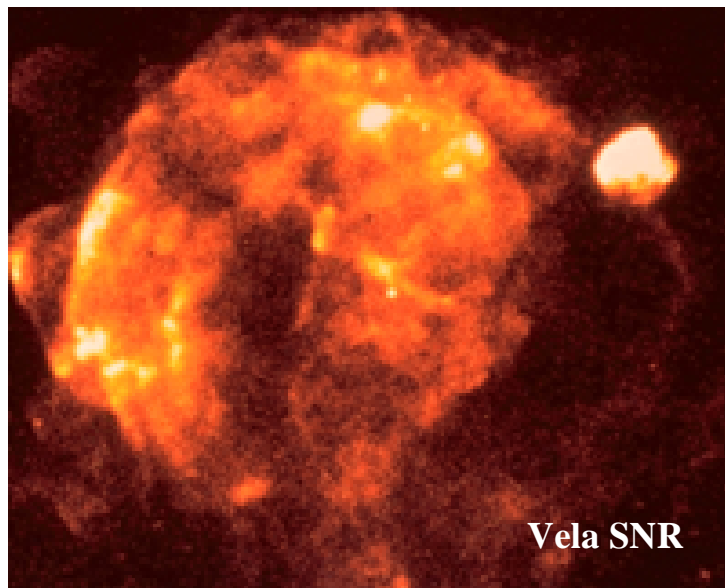
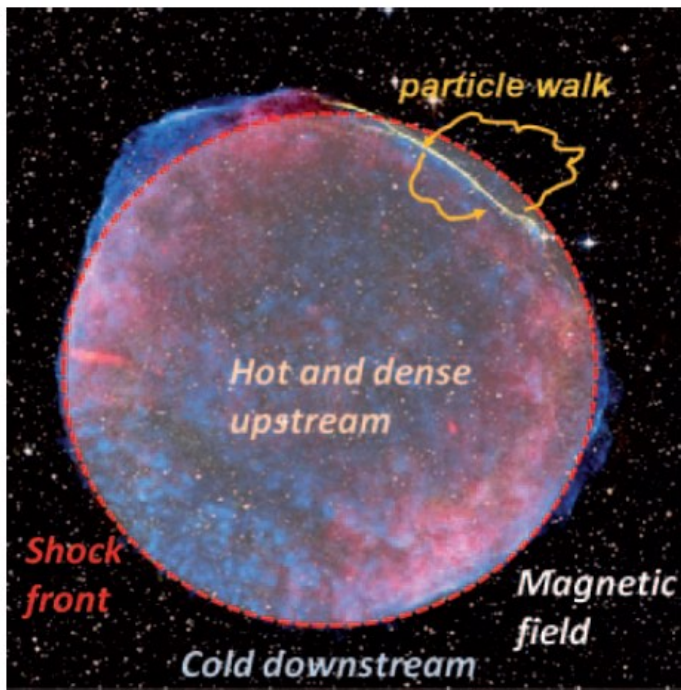


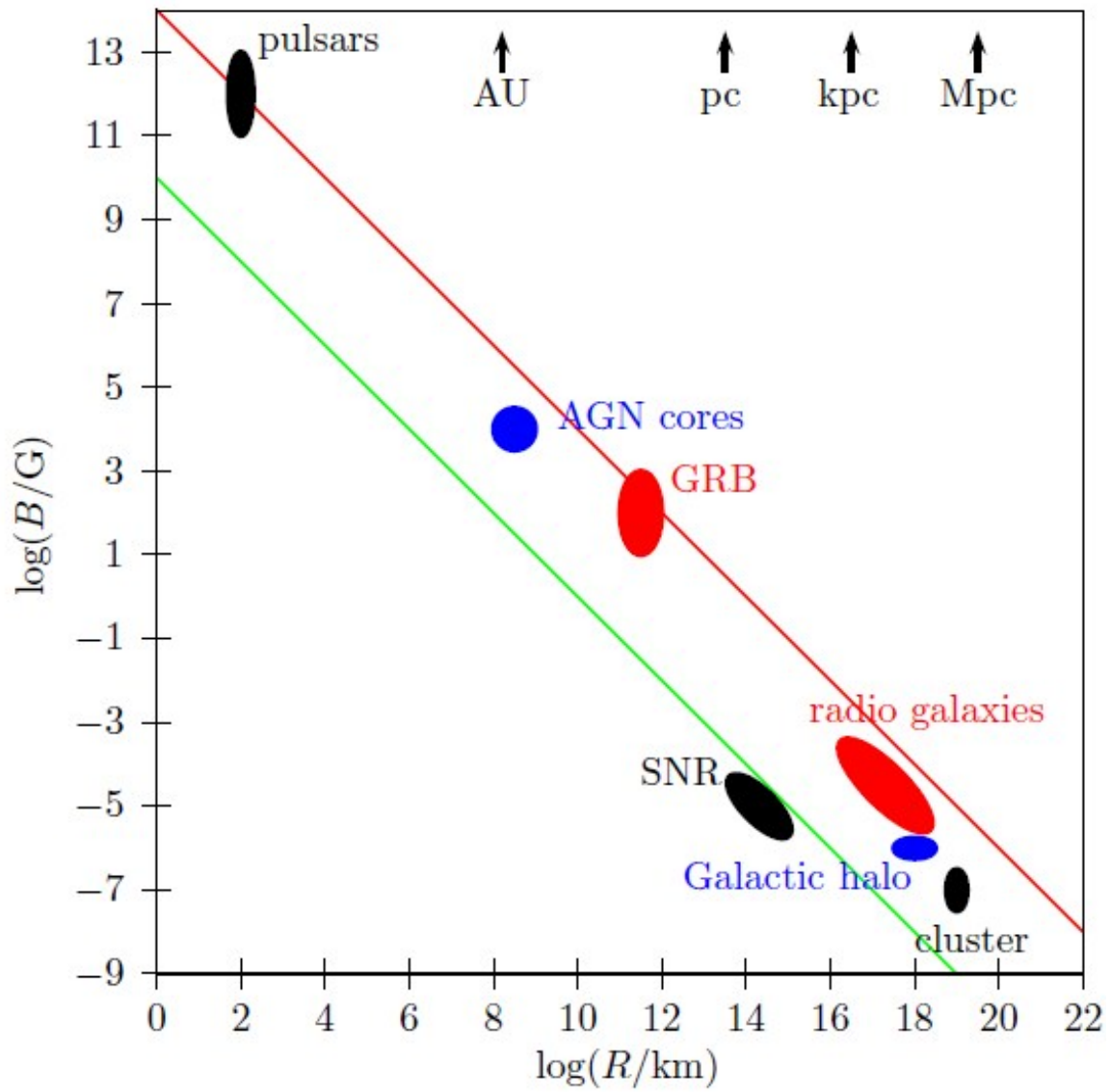
FIG. 9b

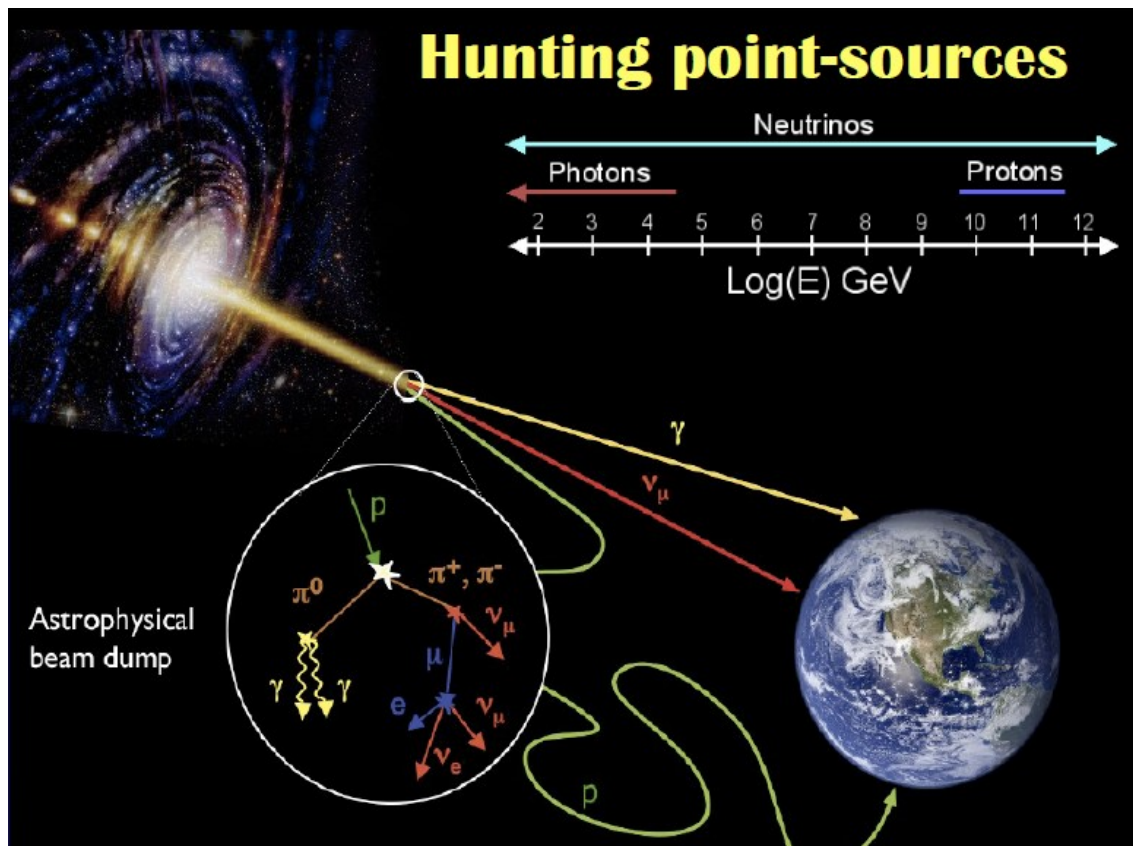
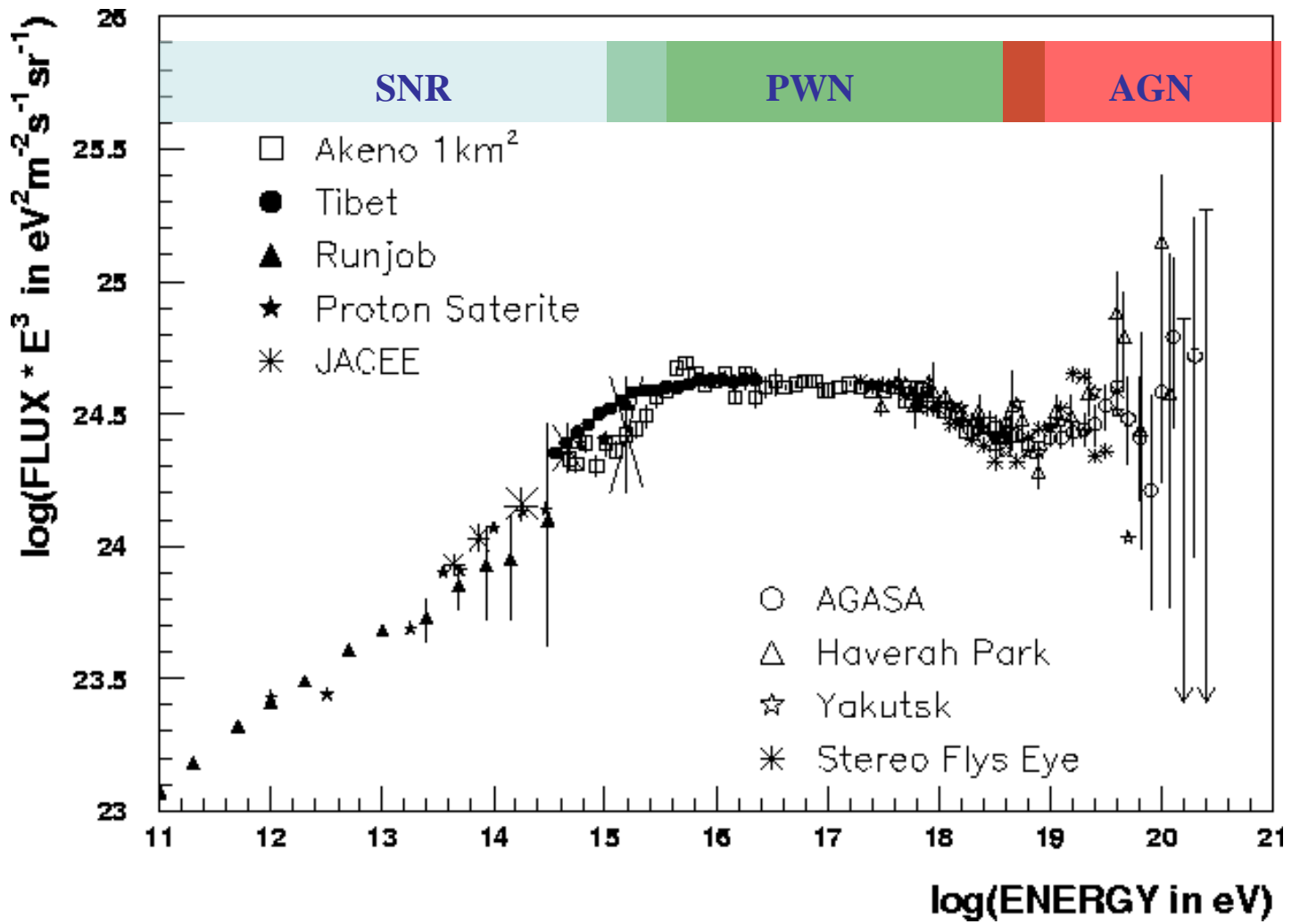
FIG. 9.—Differential energy spectra for cosmic-ray protons (a) and helium nuclei (b) measured in 1987 (filled circles for LEAP, open circles for IMP 8) along with the previous balloon measurements: open diamonds (1976 data), open squares, (1979 data), Webber et al. (1987); inverted triangles, Ryan et al. (1972); upright triangles, Smith et al. (1973). The dashed curves represent the local interstellar and modulated spectra with different amounts of modulation indicated by the modulation parameter  $\phi$ : a, local interstellar spectra (no modulation); b,  $\phi = 200$  MV; c,  $\phi = 400$  MV; d,  $\phi = 500$  MV; e,  $\phi = 600$  MV; f,  $\phi = 800$  MV; g,  $\phi = 1000$  MV.



Fisk 1979







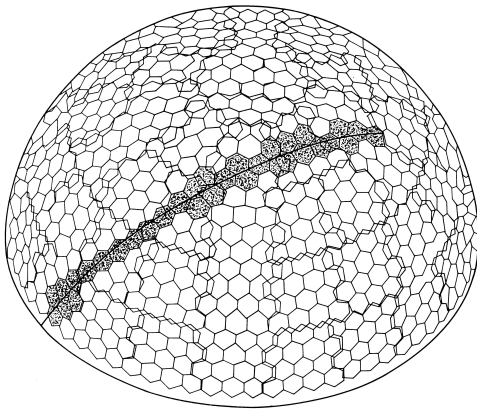
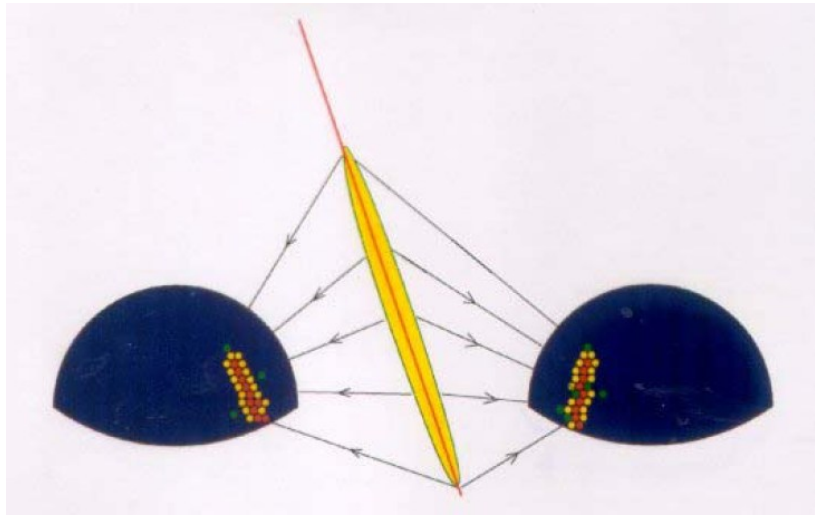


FIGURE 6.3 "Fly's Eye" phototube apertures. Shaded region represents light from EAS striking the detector. The solid line indicates the EAS trajectory across the sky.

### FLY'S EYE TECHNIQUE

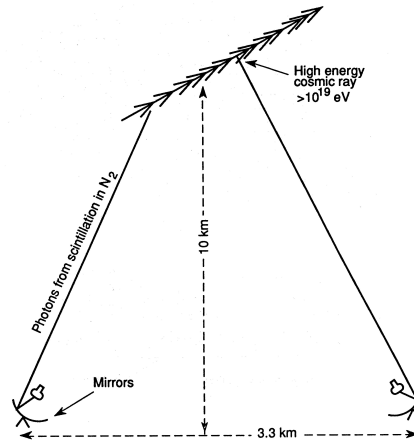


Figure 17: Fly's Eye technique [14].

### OG 10.4.9

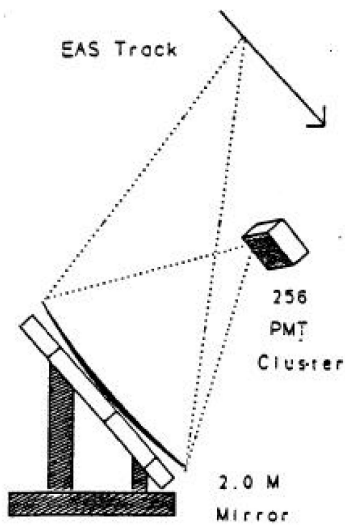


Figure 1: Single HiRes detection unit. The 2.0 m. mirror focuses nitrogen fluorescence from the EAS track onto the PMT cluster.

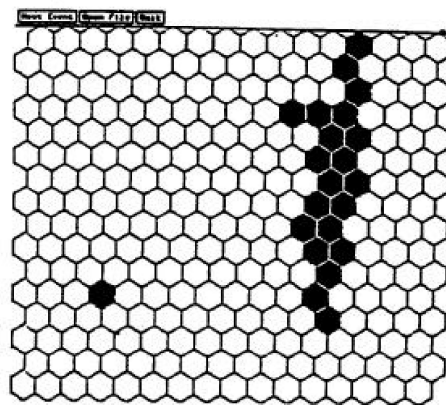
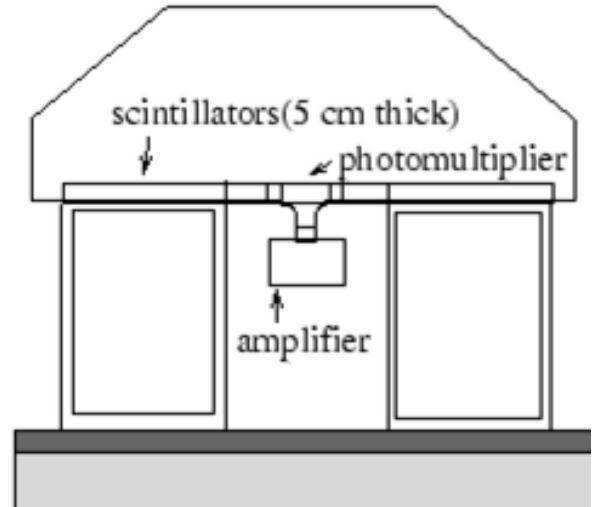
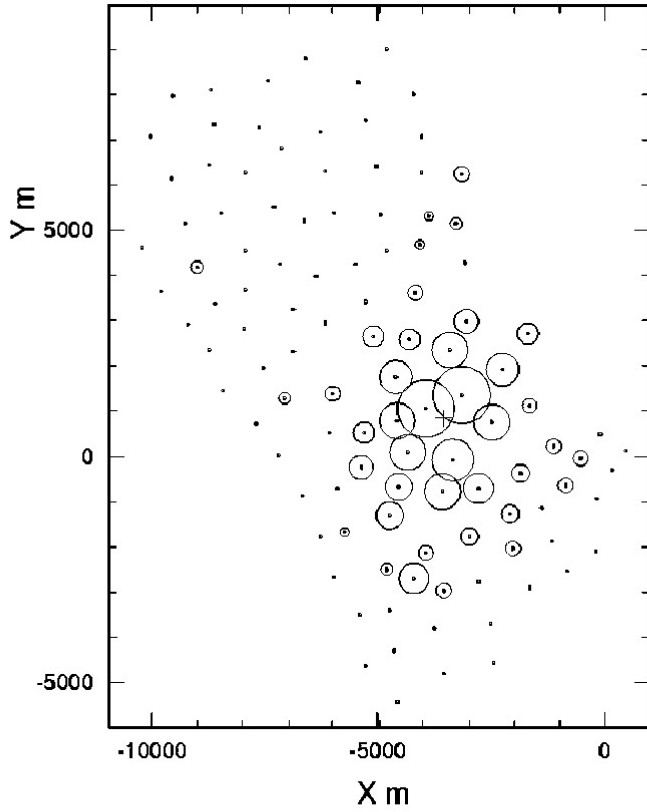
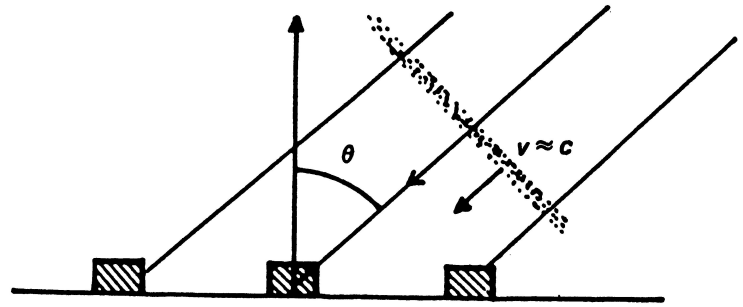
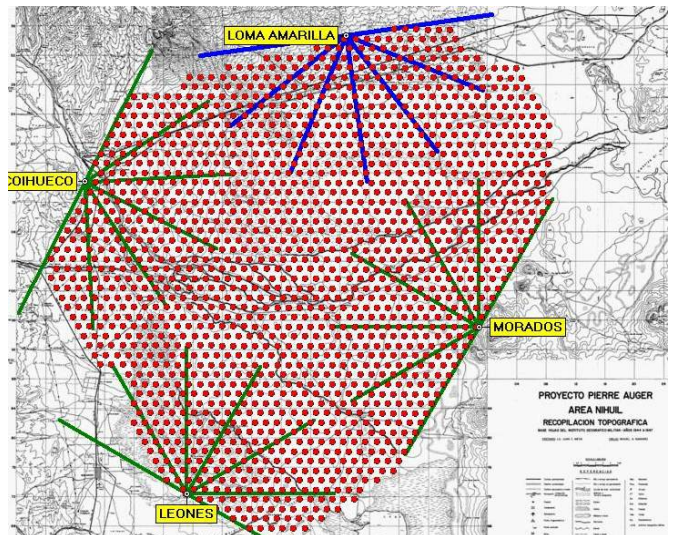
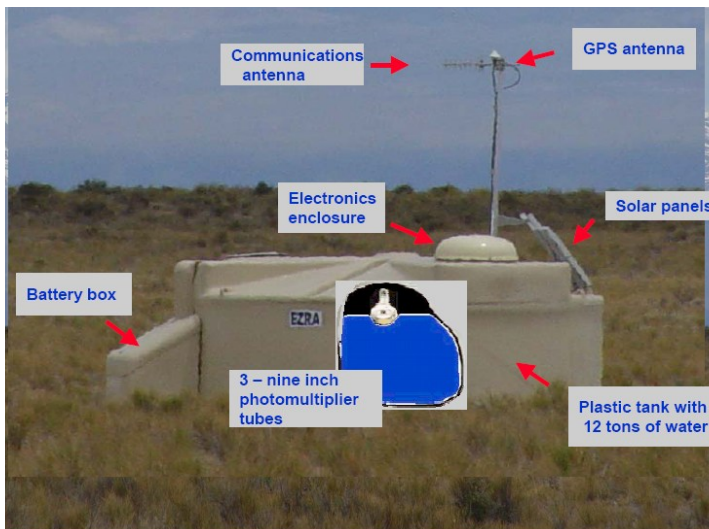


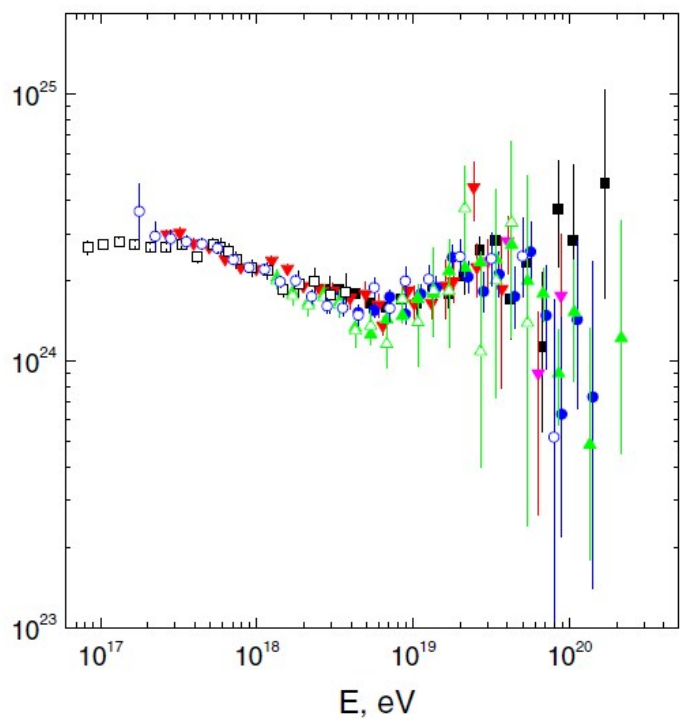
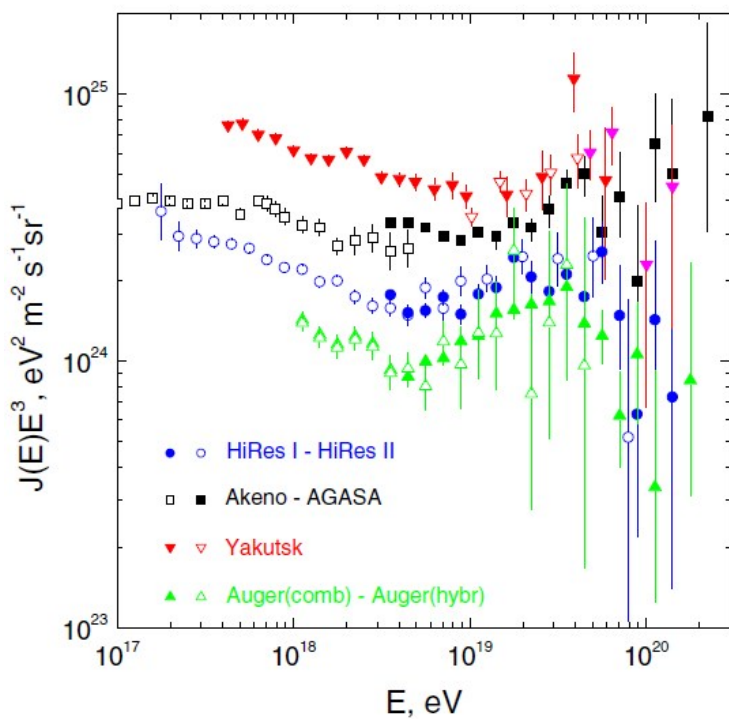
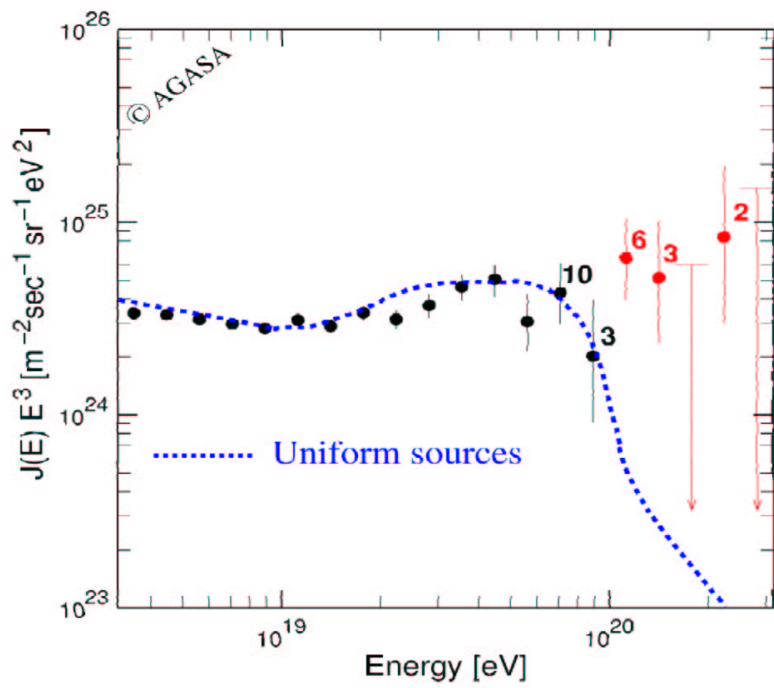
Figure 2: The first cosmic ray track observed by the prototype HiRes detector (January 20, 1991).

# AGASA



# AUGER





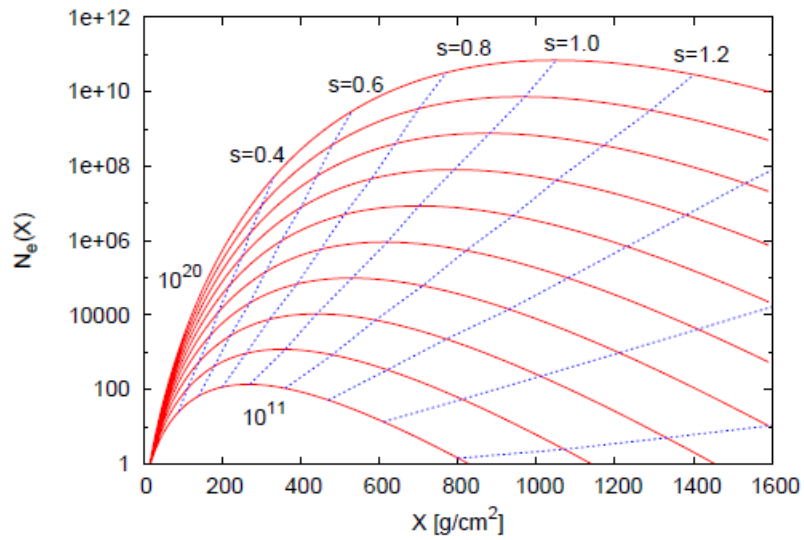
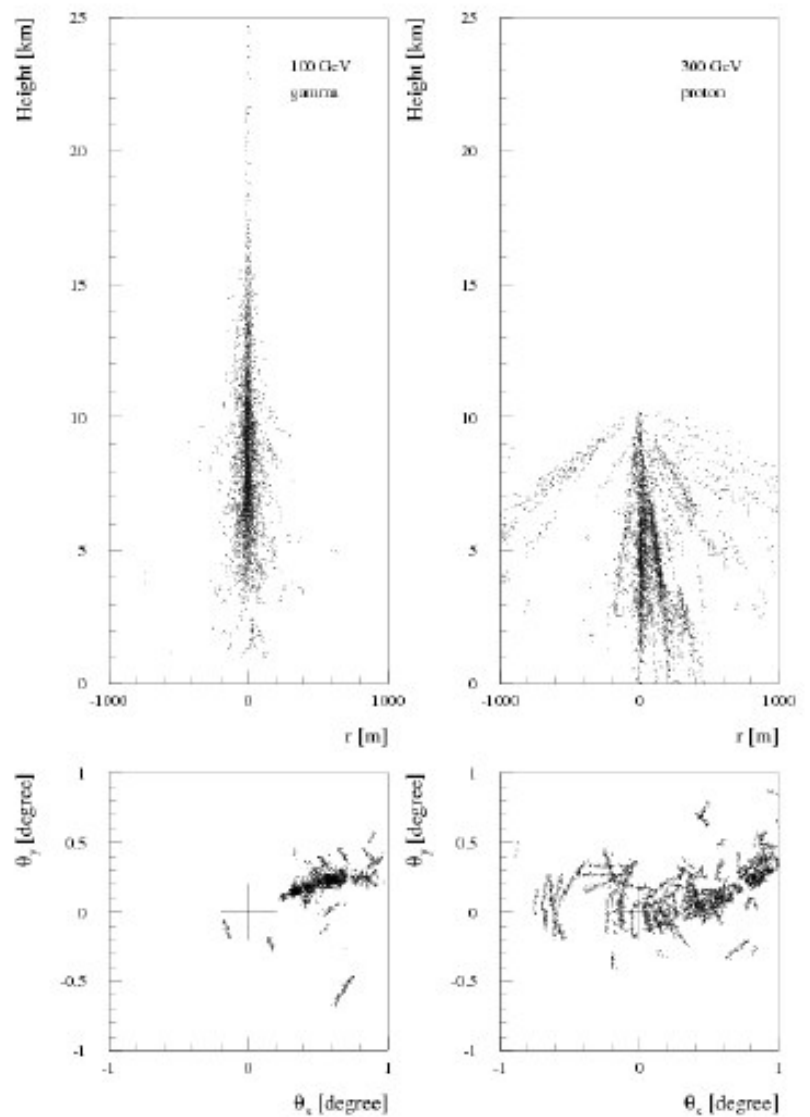


Figure 5.3: Number of electrons  $N_e(X)$  in an electromagnetic shower initiated by a photon as function of the depth  $X$  for primary energies  $10^{11}, 10^{12}, \dots, 10^{20}$  eV; the shower age  $s$  is also indicated.



This document was created with Win2PDF available at <http://www.win2pdf.com>.  
The unregistered version of Win2PDF is for evaluation or non-commercial use only.  
This page will not be added after purchasing Win2PDF.